Journal of Heredity, 2026, **117**, 566–576
https://doi.org/10.1093/jhered/esaf097
Advance access publication 21 November 2025
Genome Resources

American Genetic Association
OXFORD

Genome Resources

A chromosome level genome assembly of the marine flowering plant, Torrey's surfgrass (*Phyllospadix Torreyi*) reveals an exceptionally large Y-chromosome

Jason Johns[1,*], Malia L. Moore[2,3], Merly Escalona[4], Courtney Miller[5], Noravit Chumchim[6], Oanh Nguyen[6], Mohan P.A. Marimuthu[6], Colin W. Fairbairn[7], Eric Beraut[7], William E. Seligmann[7], Samuel Sacco[7], Erin Toffelmier[5], H. Bradley Shaffer[5], Todd P. Michael[2,3,8], Scott Hodges[1,*]

[1]Department of Ecology, Evolution, and Marine Biology, University of California, Santa Barbara, Santa Barbara, CA 93106, United States, [2]The Plant Molecular and Cellular Biology Laboratory, Salk Institute for Biological Studies, 10010 N. Torrey Pines Rd., La Jolla, CA 92037, United States, [3]Scripps Institution of Oceanography, University of California San Diego, 8622 Kennel Way, La Jolla, CA 92093, United States, [4]Department of Biomolecular Engineering, University of California, Santa Cruz, Santa Cruz, CA 95064, United States, [5]UCLA La Kretz Center for California Conservation Science, Institute of the Environment and Sustainability, University of California, Los Angeles, CA 90095, United States, [6]DNA Technologies and Expression Analysis Core Laboratory, University of California Davis, Davis, CA 95616, United States, [7]Department of Ecology and Evolutionary Biology, University of California, Santa Cruz, Santa Cruz, CA 95064, United States, [8]Department of Science and Conservation, San Diego Botanical Garden, Encinitas, CA 92024, United States

*Corresponding authors: Jason Johns, Department of Ecology, Evolution, and Marine Biology, University of California, Santa Barbara, Santa Barbara, CA 93106, USA. johnswjason@gmail.com; Scott Hodges, Department of Ecology, Evolution, and Marine Biology, University of California, Santa Barbara, Santa Barbara, CA 93106, USA. Email: sahodges@ucsb.edu

Abstract

Phyllospadix spp. (surfgrass) are flowering plants and keystone species in the rocky intertidal and subtidal environments of the North Pacific Ocean. Here we report a chromosome level assembly for *P. torreyi*, which occurs along the coast of California, sometimes in sympatry with *P. scouleri*. Both of these species and their putative hybrids are being studied as part of the California Conservation Genomics Project. *Phyllospadix* are dioecious, and males are exceptionally rare compared to females. Using high throughput, long reads (PacBio) and chromatin capture (Omni-C), we assembled a chromosome level genome for a male individual and a contig level assembly for a female individual. Comparison between the male and female assembly confirmed that the male is the heterogametic sex and has a massive Y chromosome at 124.8 megabases, which encompasses over 27% of the male genome. We also compared the male *P. torreyi* assembly to a genome from its sister genus, the monoecious *Zostera marina,* and found relatively high levels of synteny, that syntenic gene blocks on the *P. torreyi* sex chromosomes align to a single chromosome of *Z. marina,* and an estimated divergence time of ca. 25 million years ago. The *Phyllospadix* genome will be a powerful tool for studying marine dispersal, sex ratios, genetic diversity, sex chromosome evolution, and other dynamics in a keystone marine species.

Key words: dioecious, genome, intertidal, seagrass, subtidal, Y-chromosome

Introduction

Seagrasses encompass the small group of flowering plants that grow in marine environments and their habitats are considered to be one of the most human impacted ecosystems and threatened by climate change (reviewed by Mtwana Nordlund et al. 2016). Unlike most seagrasses, which form habitat in sheltered areas such as estuaries, *Phyllospadix* species (surfgrass; Zosteraceae) occur along exposed rocky coasts where they adhere to hard substrates in areas with heavy wave action. Thus, *Phyllospadix* species are particularly unusual angiosperms that form critical habitat for many organisms in the intertidal and shallow subtidal zones (Shelton 2010a).

Two species of surfgrass occur along the California coast. *Phyllospadix torreyi S. Watson* (Watson 1879) has narrow, relatively cylindrical leaves, typically makes several female inflorescences per flowering stem, and is distributed throughout California (Williams 1995; Jepson eFlora 2025. *P. scouleri* Hook has wider, flatter leaves, usually makes one female inflorescence per flowering stem, and is found more commonly from Monterey county north, although disjunct populations occur southward into Baja California (Jepson eFlora 2025). A previous study using morphological and isozyme analyses found evidence of some hybridization between the two species, but this has not been studied comprehensively (McMillan et al. 1981).

Surfgrass is dioecious, and males are exceedingly rare, often accounting for $< 10\%$ populations (Phillips 1979; Cox et al. 1992; Williams 1995; Bush et al. 2006; Shelton 2008).

Received on 26 June 2025; revised on 10 November 2025; accepted on 13 November 2025

Interestingly, (Shelton 2010b) found that sex ratios are nearly equal at the seed stage, and that the sex discrepancy only becomes pronounced in populations of established plants. While sex chromosomes have not been definitively identified cytologically (Stewart and Rudenberg 1980), genetic analysis has suggested that males are the heterogametic sex (Bush et al. 2006; Shelton 2010b). *Zostera* (Linnaeus 1753), the sister genus to *Phyllospadix*, is monoecious and a chromosome-resolved genome has been assembled for *Zostera marina* (Olsen 2016; Ma 2021). Monoecy is likely the ancestral state of seagrasses, and therefore dioecy in *Phyllospadix* likely evolved after the split with *Zostera* (Olsen 2016, Ma 2024).

The goal of the California Conservation Genomics Project (CCGP) is to make detailed assessments of genetic diversity of individuals across the tree of life and across the state, while examining the abiotic influences driving biodiversity (Shaffer et al. 2022). As such, we produced a genome assembly from a male *P. torreyi* individual with scaffolded pseudo-chromosomes. We also present an un-scaffolded female assembly to complement the male and aid in identifying Y chromosome sequence. Further, we compare the *P. torreyi* and *Z. marina* genomes to gain insight into genome divergence, including the evolution of sex chromosomes. The *Phyllospadix* genome will facilitate population and landscape genomic studies such as the CCGP and others examining the relationships of genetic diversity, population structure, and divergence with abiotic influences in intertidal plant species across California.

Methods

Biological materials

Male: We collected approximately 12 g of young leaves and floral tissue from a single subtidal individual at Campus Point in Goleta adjacent to the University of California, Santa Barbara campus (34.404861, −119.843571). Tissue was weighed, snap frozen in liquid nitrogen and stored at −80 °C.

Female: The female (Ptor311-Wns) was collected at Windansea Beach, Little Point tidepools, San Diego (32.83241, −117.28235); approximately 3 g of young leaf tissue was collected for nucleotide extraction, and flowers collected from the same individual to confirm sex. Tissue was transported in chilled sea water prior to snap freezing in liquid nitrogen for nucleotide extraction.

DNA extraction

Male

High molecular weight (HMW) genomic DNA (gDNA) was isolated from 405 mg of young leaf and floral tissues using the cetyltrimethylammonium bromide (CTAB) method as described by (Inglis et al. 2018), with the following modifications: 1) we replaced 2-mercaptoethanol (1% v/v) with sodium metabisulfite (1% w/v) in both the sorbitol wash buffer and the CTAB solution; 2) we continued washing the tissue homogenate until a clear supernatant was obtained; 3) we conducted the CTAB lysis step at 45 °C; and 4) we performed the chloroform extraction step twice using ice-cold chloroform. We evaluated DNA purity (260/280 = 1.83 and 260/230 = 2.05) using absorbance ratios measured on a NanoDrop ND-1000 spectrophotometer (Thermo Fisher Scientific, MA). The final DNA yield (7 μg total) was quantified using QuantiFluor ONE dsDNA Dye assay (Promega, WI). The size distribution of the HMW DNA was analyzed with the Femto Pulse system (gDNA 165 kb kit, Agilent, CA), revealing that 69% of the total fragments were larger than 30 kb.

Female

Leaf tissue was ground by mortar and pestle in liquid nitrogen to a fine powder, and 0.5 tsp, corresponding to approximately a 1 g tissue was carried forward to lysis. Lysis and DNA purification steps were performed in accordance with the Oxford Nanopore Technologies Community protocol for HMW DNA from Arabidopsis using the QIAGEN Blood and Cell Culture DNA Midi Kit (Qiagen,Germany; Cat# 13343) (https://community.nanoporetech.com/extraction_method_groups/plant-leaf-gDNA). To avoid sample splitting across multiple columns, the protocol was modified at the column purification step to combine two 20 mL lysis "half-reactions" on the same column. The DNA was precipitated in isopropanol for the minimum recommended incubation period of 3 hours. DNA purity and quantity was assessed by Nanodrop 2000c (Thermo Fisher Scientific; Cat# 8353-30-0011) and Qubit Fluorometer (Invitrogen, Waltham, MA; Cat# Q33238) with Broad Range Buffer (Invitrogen; Cat# Q33231), and for fragment length by Agilent 4150 Tapestation (Agilent, Santa Clara, CA; Cat# G2992AA) with a gDNA ScreenTape (Agilent; Cat# 5067–5365).

Nucleic acid library preparation

Male

The High Fidelity (HiFi) SMRTbell library was constructed using the SMRTbell prep kit 3.0 (Pacific Biosciences—PacBio, Menlo Park, CA; Cat. #102–182-700) according to the manufacturer's instructions. HMW gDNA was sheared to a target DNA size distribution between 15–18 kb using Diagenode's Megaruptor 3 system (Diagenode, Belgium; cat. B06010003). The sheared gDNA was concentrated using 1X of SMRTbell cleanup beads provided in the SMRTbell prep kit 3.0 for the repair and a-tailing incubation at 37 °C for 30 min and 65 °C for 5 min, followed by ligation of overhang adapters at 20 °C for 30 min, clean-up using 1X SMRTbell cleanup beads, and nuclease treatment at 37 °C for 15 min. The SMRTbell library was size selected using 3.1X of 35% v/v diluted AMPure PB beads (PacBio; Cat. #100–265-900) to progressively remove SMRTbell templates < 5 kb.

The Omni-C library was prepared using the Dovetail™ Omni-C™ Kit (Dovetail Genomics, Scotts Valley, CA) according to the manufacturer's protocol with slight modifications. First, specimen tissue (young leaves) was thoroughly ground with a mortar and pestle while cooled with liquid nitrogen. Nuclear isolation was then performed using published methods (Workman et al. 2018). Subsequently, chromatin was fixed in place in the nucleus and digested under various conditions of DNase I until a suitable fragment length distribution of DNA molecules was obtained. Chromatin ends were repaired and ligated to a biotinylated bridge adapter followed by proximity ligation of adapter containing ends. After proximity ligation, crosslinks were reversed and the DNA was purified from proteins. Purified DNA was treated to remove biotin that was not internal to ligated fragments. An NGS library was generated using an NEB Ultra II DNA Library Prep kit (New England Biolabs, Ipswich, MA) with an Illumina compatible y-adaptor. Biotin-containing fragments

were then captured using streptavidin beads. The post capture product was split into two replicates prior to PCR enrichment to preserve library complexity with each replicate receiving unique dual indices.

Female

For sequencing on a PacBio Revio, a HiFi SMRTbell library was constructed and barcoded using the HiFi SMRTbell prep kit 3.0 (PacBio, Cat. #102–182-700) according to the manufacturer's instructions and the same as the male *P. torreyi* library preparation.

DNA sequencing

Male

The 15–18 kb average HiFi SMRTbell library was sequenced at the UC Davis DNA Technologies Core (Davis. CA) on a PacBio Sequel IIe sequencer using one 8 M SMRT cell (PacBio, Menlo Park, CA; Cat #101–389-001 with Sequel II sequencing chemistry 2.0 and 30-h movies. The Omni-C library was sequenced at Vincent J. Coates Genomics Sequencing Lab (Berkeley, CA) on an Illumina NovaSeq 6000 platform (Illumina, San Diego, CA) to generate approximately 100 million 2 × 150 bp read pairs per GB genome size.

Female

For the female (Ptor311-Wns), the SMRTbell library was multiplexed with one other library and run on a PacBio Revio running instrument chemistry bundle v13.0.0.205983 with a 25 M Single Molecular Real-Time (SMRT) cell (PacBio, Cat# 102–202-200) and 30-h movie time.

Genome size estimation

We estimated the genome size of *P. torreyi*, first by flow cytometry. We collected young tissue from two plants near Campus Point at the UCSB campus and shipped them on ice to the laboratory of Brian Husband (University of Guelph, Guelph, ON Canada) for analysis using the methods of Sabara et al. 2013 and *Sorghum bicolor* as a standard. Plants were not flowering at the time and given the highly female biased sex ratio of natural populations were very likely female individuals. We also estimated the genome sizes of both the male and female samples for genome sequencing using their K-mer frequency distribution with the long read PacBio, SMRT, HiFi reads (Supp. Figs. S2, S3).

Nuclear genome assembly

Male

We assembled the genome of the male *P. torreyi* following the CCGP assembly pipeline, which uses PacBio HiFi reads and Omni-C data to produce high quality and highly contiguous genome assemblies. The pipeline is outlined in Table S1 and lists the tools and non-default parameters used in the assembly process. First, we removed the remnants adapter sequences from the PacBio HiFi dataset using HiFiAdapterFilt (Sim et al. 2022) and generated the initial phased diploid assembly using HiFiasm (Cheng et al. 2021) on Hi-C mode, with the filtered PacBio HiFi reads and the Omni-C dataset. We aligned the Omni-C data to both assemblies following the Arima Genomics Mapping Pipeline (https://github.com/ArimaGenomics/mapping_pipeline) and then scaffolded both assemblies with SALSA (Ghurye et al. 2017; Ghurye et al. 2019).

Assemblies were manually curated by iteratively generating and analyzing their corresponding Omni-C contact maps. To generate the contact maps we aligned the Omni-C data with BWA-MEM (Li 2013), identified ligation junctions, and generated Omni-C pairs (Lee et al. 2022) using pairtools (Open2C et al. 2024). We generated a multi-resolution Omni-C matrix with cooler (Abdennur and Mirny 2020) and balanced it with hicExplorer (Ramírez et al. 2018). We used HiGlass (Kerpedjiev et al. 2018) and the PretextSuite (https://github.com/wtsi-hpag/PretextView; https://github.com/wtsi-hpag/PretextMap; https://github.com/wtsi-hpag/PretextSnapshot) to visualize the contact maps where we identified misassemblies and misjoins, and finally modified the assemblies using the Rapid Curation pipeline from the Wellcome Trust Sanger Institute, Genome Reference Informatics Team (https://gitlab.com/wtsi-grit/rapid-curation). Some of the remaining gaps (joins generated during scaffolding and/or curation) were closed using the PacBio HiFi reads and YAGCloser (https://github.com/merlyescalona/yagcloser). Finally, we checked for contamination using the BlobToolKit Framework (Challis et al. 2020).

Female

We assembled the female *P. torreyi* genome (Ptor311-Wns) with HiFiasm v0.19.9-r616 using the PacBio HiFi reads (Cheng et al. 2021). We report the primary output, which is an un-phased consensus assembly. The assembly was passed through the National Center of Biotechnology Information's (NCBI) Foreign Contamination Screening—GX Program v0.5.0 (https://github.com/ncbi/fcs-gx) to remove contaminant contigs, given NCBI Taxonomy ID 55486 for *P. torreyi* (Astashyn et al. 2024).

Genome quality assessment

We generated k-mer counts from the PacBio HiFi reads using meryl (https://github.com/marbl/meryl). The k-mer counts were then used in GenomeScope2.0 (Ranallo-Benavidez et al. 2020) to estimate genome features including genome size, heterozygosity, and repeat content. For contiguity metrics, we ran QUAST (Gurevich et al. 2013). To evaluate genome quality and functional completeness we used BUSCO (Manni et al. 2021a) with the Embryophyta ortholog database (embryophyta_odb10) which contains 1614 genes. Assessment of base level accuracy (QV) and k-mer completeness was performed using the previously generated meryl database and merqury (Rhie et al. 2020). We further estimated genome assembly accuracy via BUSCO gene set frameshift analysis using the pipeline described in (Korlach et al. 2017). Measurements of the size of the phased blocks is based on the size of the contigs generated by HiFiasm on HiC mode. We follow the quality metric nomenclature established by (Rhie et al. 2021), with the genome quality code x.y.P.C, where, x = log10[contig NG50]; y = log10[scaffold NG50]; P = log10[phased block NG50]; C = % genome represented by the first "n" scaffolds, following a karyotype of 2n = 12, for this species according to Genome on a Tree [GoaT; tax_tree(*P. torreyi*); (Challis et al. 2023)]. Quality metrics for the notation were calculated on the primary haplotype assembly.

Chloroplast genome assembly

The chloroplast sequence for *P. torreyi* was generated with Oatk (Zhou et al. 2024). We used GeSeq (Tillich et al. 2017) to generate a draft genome annotation and after completion of the male nuclear genome assembly. We used the chloroplast genome assembly from *Arabidopsis thaliana*

[NCBI:NC_000932.1; (Sato et al. 1999)] to visually validate order of the regions. For this inspection, we aligned the generate sequence against the guide, using lastz (Harris 2007), extracted contigs and fixed orientation when needed using samtools (Danecek et al. 2021) and seqtk (https://github.com/lh3/seqtk). Visual validation of the alignment was done using LAJ (Wilson et al. 2001). The resulting assembly was annotated using the online version of GeSeq (Tillich et al. 2017) and visualized using the online version of OGDRAW (Greiner et al. 2019). After completion of the nuclear genome, we searched for matches of the resulting chloroplast assembly sequence in the nuclear genome assembly using BLAST+ (Camacho et al. 2009) and filtered out contigs and scaffolds from the nuclear genome with a percentage of sequence identity > 99% and size smaller than the chloroplast assembly sequence.

Evaluating the assembly

We used BUSCO (Manni et al. 2021b) with the embryophyta database (embryophyta_odb10) to evaluate genome quality and functional completeness, and compared the results to those obtained from the most recent *Z. marina* v.3.1 genome assembly (Ma et al. 2021). To assess broad synteny and genome structure we generated dot plots with D-Genies using Minimap version 2, and the "hide noise" feature (Cabanettes and Klopp 2018).

Coverage analysis and heterozygosity calls

For the coverage analysis we generated tracks for depths of coverage for both male and female samples by aligning their corresponding PacBio HiFi datasets to the male genome assembly (laPhyTorr1.0.p). In detail, we use minimap2 (−ax map-hifi) (Li 2018; Li 2021), subsequently sorted and converted the alignments into BAM files using samtools sort (Danecek et al. 2021). From the resulting files, we generated per window coverage information using the module genomecov of bedtools (−bga, −split) (Quinlan and Hall 2010). In addition, we ran a genome mappability analysis to understand the complexity of the genome using GenMap (k = 150, e = 0) (Pockrandt et al. 2020).

For the heterozygous calls, we used the BAM files from the coverage analysis and called variants using DeepVariant (Poplin et al. 2018), then per alignment calculated the number of segregating sites and heterozygous calls in 10 kb windows. Finally, we aggregated all the information from coverage and heterozygous calls and visualized it using HiGlass (Fig. S1).

Annotating genes and defining orthologs to *Z. Marina*

We annotated protein coding genes on all putative autosomes and sex chromosomes in the male assembly with the machine learning gene prediction tools Helixer v0.3.3 (Stiehler et al. 2020) and eggNOG mapper (Cantalapiedra et al. 2021). The JCVI toolkit v1.5.3 Python implementation of MCscan (Wang et al. 2024) was used to identify syntenic ortholog pairs between male *P. torreyi* and *Z. marina* v.3.1 (Ma et al. 2021). We used default parameters for jcvi.compra.catalog (−-cscore 0.7, −-identity 90, −-coverage 70) to define orthology by blast similarity and alignment coverage, and jcvi.compra.synteny (−-gap_size 30, −-match_size 5 –score_cutoff 25, −-span_size 30) to define syntenic blocks, used for plotting genome macrosynteny between *P. torreyi* and *Z. marina* in Fig. 3B. These parameters were sufficiently relaxed as to capture a large number of syntenic gene pairs despite the evolutionary distance between the two organisms (diverged protein sequences), and allowed for syntenic blocks containing up to 30 non-syntenic genes to maintain synteny visualization across regions with some tandem duplications and insertions.

Estimating speciation divergence time

All syntenic orthologs between *P. torreyi* and *Z. marina* were supplied to gKaKs v1.3.0 (Zhang et al. 2013) to compute divergence values, except orthologs on the Y and X, as they have different divergence rates due to several factors. To estimate speciation divergence time between *Z. marina* and *P. torreyi* we used the neutral substitution rate of 6.5e-09 per synonymous site per year for the grass monocot *Oryza sativa* (Gaut et al. 1996).

Results

P. torreyi genome size estimation

There are no published genome size estimates for *P. torreyi*. The mean genome size estimates from flow cytometry for the two samples (each analyzed with two replicate runs) were 333.5 Mbp and 330.1 Mbp. The k-mer analysis of the male genome yielded an estimate of 356 megabases (Mb) with 0.78% heterozygosity. The k-mer spectrum shows a bimodal distribution with a major peak at ∼90-fold coverage and a minor peak at ∼45-fold coverage (Fig. 2A). The female genome was estimated to be 289 Mb with 2.91% heterozygosity rate. The k-mer spectrum shows a bimodal distribution with a major peak at ∼60-fold coverage and a minor peak at ∼120-fold coverage (Fig. S3). "Based on the k-mer analyses, the male genome was 23% (67Mb) larger than the female genome, likely due to the Y-chromosome."

Nuclear genome assembly

We generated PacBio long read data for both male and female samples to generate high quality genome assemblies. For the male, we generated ∼97X genome coverage of PacBio HiFi reads with a N50 read length of 16 364 bp; in addition, for the male we generated a Omni-C High-throughput Chromatin Conformation and Capture (HiC) to scaffold the contigs into chromosomes (Table S2).

The final genome assembly (laPhyTorr1) consists of two phased haplotypes; however, the assemblies have been tagged as primary and alternate based on our assessment of completeness and contiguity. The primary haplotype (laPhyTorr1.0.p) consists of 79 scaffolds spanning 447.94 Mb with a contig N50 length of 21.57 Mb, a scaffold N50 length of 36.62 Mb, the largest contig size of 37.77 Mb, and the largest scaffold size of 124.81 Mb (Table 1, Table S2). SCAF_8 of the primary male assembly did not have a homologous scaffold in the alternate haplotype of the male assembly, but it did align to contig ptg000002l in the female consensus assembly. Thus, SCAF_8 was included in the primary male haplotype.

The alternate haplotype (laPhyTorr1.0.a) consists of 47 scaffolds spanning 263.66 Mb with a contig N50 length of 25.23 Mb, a scaffold N50 length of 33.46 Mb, the largest contig size of 35.93 Mb and the largest scaffold size of 40.26 Mb (Table 1, Table S2).

The primary haplotype has a BUSCO completeness score for the Embryophyta gene set of 93.5%, a base pair quality

Table 1. Basic assembly metrics for the male assembly (both haplotypes) and the contig-level female assembly.

	Total size	Contig N50	Scaffold N50	BUSCO completeness
Male (primary)	447.9 Mb	21.6 Mb	36.6 Mb	93.5%
Male (alternate)	263.7 Mb	25.2 Mb	33.5 Mb	79.3%
Female	355.8 Mb	32.3 kb	NA	94.9%

value (QV) of 71.55, a k-mer completeness of 90.74%, and a frameshift indel QV of 49.45 (Table 1, Table S2). The alternate haplotype has a BUSCO completeness score for the same gene set of 79.3%, a base pair QV of 70.65, a k-mer completeness of 72.2%, and a frameshift indel QV of 48.84. Because the assemblies differ in chromosome content, their relative completeness cannot be directly compared. To assess the relative completeness of the haplotype assemblies of the male, we removed Pt.1 (Y), Pt.5 (X) and Pt.8 from the primary assembly and found a BUSCO completeness of 76.5%, similar to the alternate assembly (79.3%). Similarly, to assess relative completeness of the male and female assemblies, we removed Pt.1 (Y) from the male primary assembly and found a BUSCO completeness of 92.1%, similar to the female assembly (94.9%).

During manual curation we made a total of 34 joins (27 on the primary haplotype and 7 on the alternate haplotype) and 4 breaks (2 per haplotype) based on the signal from the Omni-C contact maps. We filtered out a total of 76 contigs on the contamination screening with Blobtools corresponding to various contaminants (detailed taxonomic assignment of removed contigs on Table S3). We also filtered out 1 contig corresponding to a mitochondrial contamination and 11 contigs corresponding to chloroplast contamination. No other contigs were removed.

The Omni-C contact maps show highly contiguous assembly, suggesting that the *P. torreyi* genome is organized in 11 chromosomes based on the number of major bins along the diagonal axis of the plot (Fig. 2B). Due to the ease of analysis and the substantially higher completeness of the primary assembly, we placed both the putative Y and X chromosomes on the primary assembly. Assembly statistics are reported in Table S2 and represented graphically in Fig. 2C and D. We have deposited both haplotypes of the genome assembly on NCBI GenBank (see Table S2 and Data availability for details).

For the female, we generated 117X coverage and assembled a 355.8 Mb consensus, contig-level assembly (Ptor311-Wns) with a contig N50 length of 32.3 Mb and BUSCO completeness of 94.9% (Table 1, Table S2).

Chloroplast genome assembly

The final chloroplast assembly of *P. torreyi* is 123,576 bp long, 36.15% GC content. The large single copy is 85,734 bp long, the small single copy is 17,665 bp long, and the inverted repeat is 24,692 bp long. This plastome contains a total of 270 genes including rRNAs and tRNAs (not counting the duplication of the IR). We have deposited the chloroplast genome assembly on NCBI GenBank (see Data availability for details).

Comparison of male and female assemblies

Going forward, we refer to chromosomes, scaffolds or contigs by the species (Pt, *P. torreyi*; or Zm, *Z. marina*) followed by their number, e.g, chromosome 1 in *P. torreyi* is Pt.1. Chromosomes were named/numbered according to their size, where chromosome 1 is the largest, regardless of whether they were subsequently determined to be sex chromosomes. Unless specified, we refer to the primary assembly of the male sample.

Dot plots between the two haplotypes of the male assembly revealed that three large scaffolds in the primary assembly (Pt.1, Pt.5, and Pt.8) did not have a homologous counterpart in the alternate assembly (Fig. S4), suggesting that they may be hemizygous. However, coverage of PacBio HiFi reads from both the male and female samples to the primary assembly showed similar coverage to Pt.8 as for most other large scaffolds, indicating that Pt.8 is an autosome that did not resolve into separate haplotypes in our analysis, possibly due to a lack of variation between haplotypes (Fig. S1). Conversely, reads from the male sample had less than about one-half the coverage on Pt.1 and Pt.5 as on autosomes, indicating hemizygosity. Using the female reads, Pt.1 had essentially no coverage except for a ca. 5 Mb region at one end, and Pt.5 had similar coverage to other autosomes (Fig. S1). In addition, dot plots between the male primary assembly and the female consensus assembly show high sequence similarity between Pt.5 and Pt.3 of the female assembly. Further, the 5 Mb region at one end of Pt.1 is highly similar to and contiguous with the sequence at one end of Pt.5 (Pt.3 in the female assembly, Fig. 3A). Thus, given that Pt.1 appears to be hemizygous in the male and non-existent in the female (other than the ca. 5 Mb region), it is the putative Y chromosome. Further, as Pt.5 appears to be hemizygous in the male, yet have two copies in the female, it is the putative X-chromosome. The ca. 5 Mb region that is both homologous and contiguous on both Pt. 1 and Pt. 5 is the putative pseudoautosomal region (PAR), while the remaining 99 Mb of Pt.5 is the sex determining region (SDR).

The *P. Torreyi* Y chromosome

The *P. torreyi* Y chromosome (Pt.1) is unusually large at 124.8 Mb, or 27% of the haploid genome. Like other plant Y chromosomes, it is gene-poor; we annotate just 581 protein-coding genes (3% of all predicted genes; Fig. S1). Using read-coverage, gene density, and X–Y collinearity with the X chromosome (Pt.5), we delimit a PAR of ~ 5 Mb (4% of Pt.1) and a sex-determining region (SDR) comprising the remainder (Fig. 3A). The PAR contains 209 predicted genes and the SDR 372; 141 PAR genes and 106 SDR genes retain X–Y synteny. Nonsynonymous/synonymous divergence (Ka/Ks) is elevated in both the PAR and the SDR of the Y, at approximately two-times the X and autosomal values, consistent with reduced efficacy of purifying selection (Fig. S5).

As a preliminary analysis, we scanned the list of functional annotations for genes of interest for the origin of dioecy such as genes involved in floral or gamete development (Table S4). For example, genes with high similarity to those involved

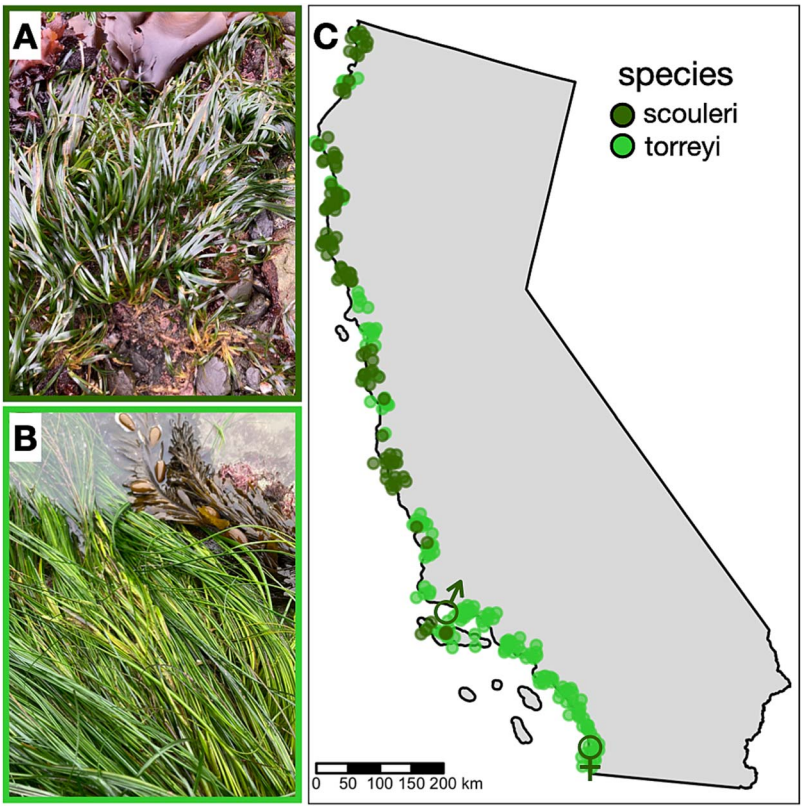

Fig. 1. Photographs and ranges of *Phyllospadix* (surfgrass) species. A) *P. scouleri* and B) *P.* (male individual with inflorescences). Border colors around photos in A & B correspond to the color of the dots in C. C) Map of California showing the locations of sites for both species of *Phyllospadix* found in coastal California visited by the authors. The collection points of *P. Torreyi* tissue used for the male (♂) and female (♀) genome assemblies are indicated.

with floral development (*APETALA1* and *CONSTITUTIVE TRIPLE RESPONSE1*), the development of the central cell of the female gametophyte (*AGAMOUS-like80*), and meiotic division (*MEIOSIS-DEFICIENT2*). Thus, this system will likely add significantly to our knowledge of sex chromosome evolution.

Comparison of *P. Torreyi* to *Z. Marina*

We visualized how orthologous genes have moved between chromosomes, contributed to chromosome fusions or splits, and undergone large structural inversions by extracting syntenic gene blocks between *P. torreyi* and *Z. marina*. From these syntenic blocks, 301 were plotted to create the linear karyotype plot in Fig. 3B. This comparison revealed two chromosomes with highly conserved synteny, Zm.2 and Zm.4 corresponding to Pt.2 and Pt.6, respectively. Some noticeable rearrangements and splits/fusions have also taken place as these plants diverged. Two *Z. marina* chromosomes share their syntenic blocks with nearly all the blocks from two *P. torreyi* chromosomes: (Zm.3 with Pt.7 and Pt.8) and (Zm.6 with Pt.9 and Pt.10). Finally, two *Z. marina* chromosomes share all their syntenic blocks with blocks from two *P. torreyi* chromosomes plus the blocks from one end of a third *P. torreyi* chromosome: (Zm.1 with Pt.11, Pt.3 and one end of Pt.4) and [Zm.5 with the sex chromosomes Pt.5 (X), Pt.1 (Y) and the other end of Pt.4].

Computing synonymous divergence values for 9378 orthologous protein pairs from syntenic blocks, excluding those on the sex chromosomes, indicates that *P. torreyi* and *Z. marina* diverged from a common ancestor approximately 25 million years ago (Mya). Of the 581 annotated proteins on the *P. torreyi* Y, 112 are in syntenic blocks shared with *Z. marina*. There are 81 syntenic genes in the PAR, while there are 31 in the SDR; five have two copies left over from the last whole genome duplication. 37 syntenic genes in the PAR are mitochondrial insertions, while the remaining 75 genes (44 PAR, 31 SDR) are syntenic with Zm.5.

Discussion

Here we present the first de novo genome for one of the keystone species of the California coastal intertidal and subtidal habitats, *P. torreyi*. As *P. torreyi* is dioecious, we have assembled genomes from both male and female individuals. Comparing these genomes revealed that the male is the heterogametic sex, with a putative X chromosome, a very large putative Y chromosome, and 9 major autosomal chromosomes. This scaffold number ($n = 10$) matches the chromosome number identified with cytological analysis (Harada 1944), which is also the ancestral chromosome number of the Zosteraceae (Silva et al. 2021).

Notably, the putative Y chromosome (Pt.1) is extremely large at 124.8 Mb, which is over 27% of the size of the entire haploid genome. A similar pattern was recently found in *Silene latifolia*, where the Y chromosome consists of ca. 20% of the total genome (Moraga et al. 2025, Akagi et al. 2025). Other recent genome assemblies for dioecious plants have revealed large and/or degenerate Y chromosomes (e.g. *Rumex hastatulus*: Sacchi et al. 2024; *Spinacia tetranda*: She et al. 2025). As is common with Y chromosomes, Pt.1 is very

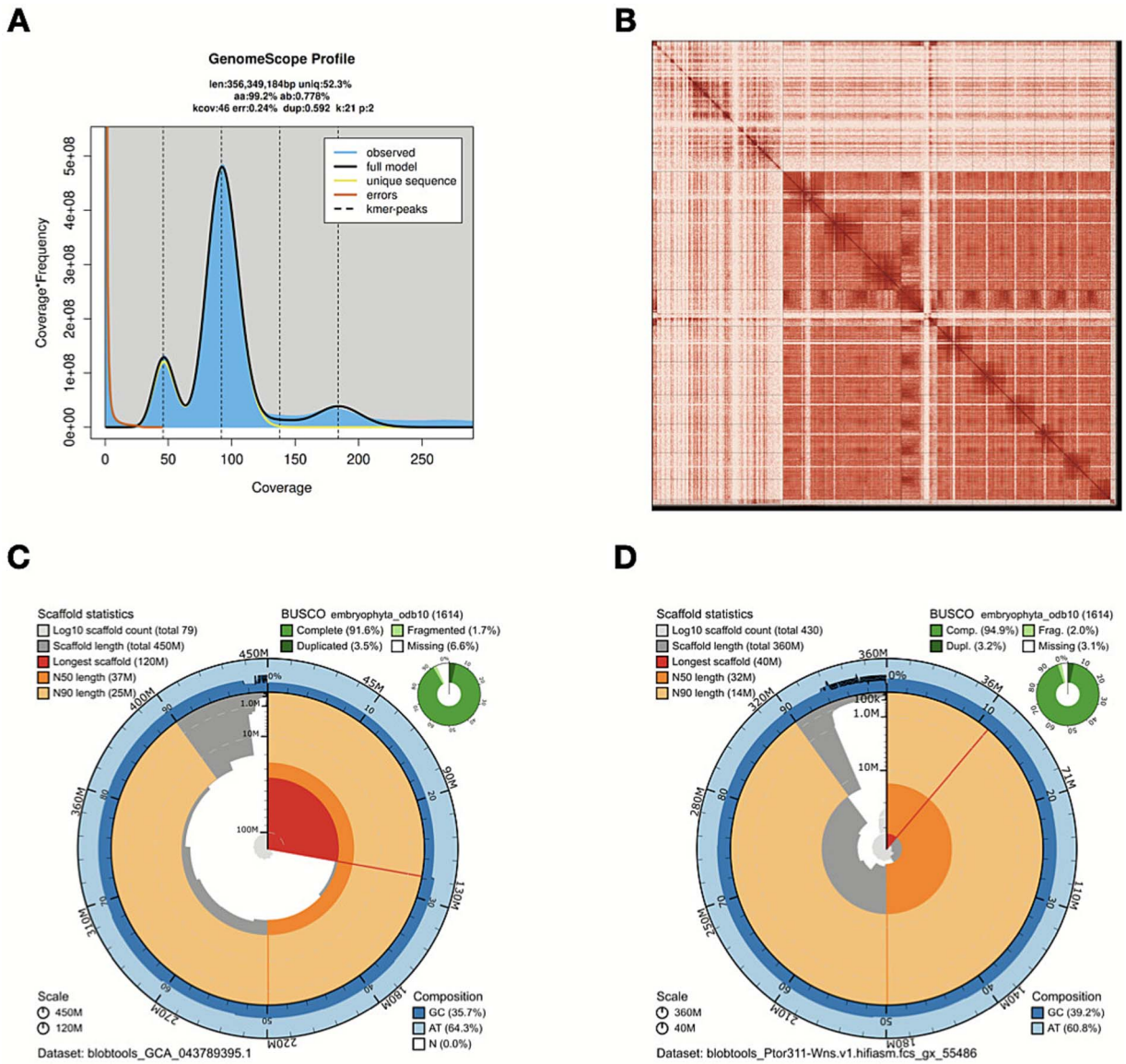

Fig. 2. Overview of genome assembly metrics for *P. Torreyi*. A) K-mer spectrum output of male PacBio HiFi data without adapters, generated using GenomeScope2.0. K-mers at lower coverage and lower frequency correspond to differences between haplotypes, whereas the higher coverage and higher frequency k-mers correspond to the similarities between haplotypes. B) Hi-C contact map for the primary genome assembly of the male genome generated with PretextSnapshot. Hi-C contact maps translate proximity of genomic regions in 3-D space to contiguous linear organization. Each cell in the contact map corresponds to sequencing data supporting the linkage (or join) between two of such regions. Scaffolds are separated by black lines and higher density corresponds to higher levels of fragmentation. C,D) Snail plots for the primary (C) male and consensus (D) female genome assembly showing a graphical representation of the quality metrics in Table S2 for the primary assembly. The circle represents the full size of the assembly. From the inside-out, the central plot displays length-related metrics. The red line represents the longest scaffold; other scaffolds are ordered by size moving clockwise around the plot and drawn in gray starting from the outside of the central plot. Dark and light orange arcs mark the scaffold N50 and N90 values. The central light gray spiral shows the cumulative scaffold count with a white line at each order of magnitude. White regions in this area reflect the proportion of ns in the assembly the dark versus light blue area around it shows mean, maximum, and minimum GC versus AT content at 0.1% intervals (Challis et al. 2020).

gene poor (Charlesworth and Charlesworth 2000; Bachtrog 2013), with only 581 annotated genes, 209 of which are in the PAR, and only makes up ca. 4% of the chromosome.

We would expect the hemizygous Y chromosome (Pt.1) to have about half of the coverage as the autosomes in the male. In this assembly, however, the male had less than half of the coverage on this chromosome compared to the autosomes, and about half of the coverage in the PAR (Fig. 1). This is likely due to lower mappability and the gene poor nature of Pt.1, which may be caused by high levels of repetitiveness on this chromosome, possibly due in part to an accumulation of transposable elements (Fig. 1). Further, the X chromosome, which has higher gene content and thus mappability, has closer to half the coverage, as expected for a hemizygous chromosome.

Syntenic blocks of homologous genes between *P. torreyi* and *Z. marina* revealed significant rearrangements (Fig. 3B). Previous phylogenetic analysis of chromosome number evolution in marine angiosperms found that $n = 10$ is the ancestral state and that a series of chromosomal fusions must have led to a reduction from $n = 10$ in the common ancestor of the Zosteraceae to $n = 6$ in *Zostera* (Silva et al. 2021).

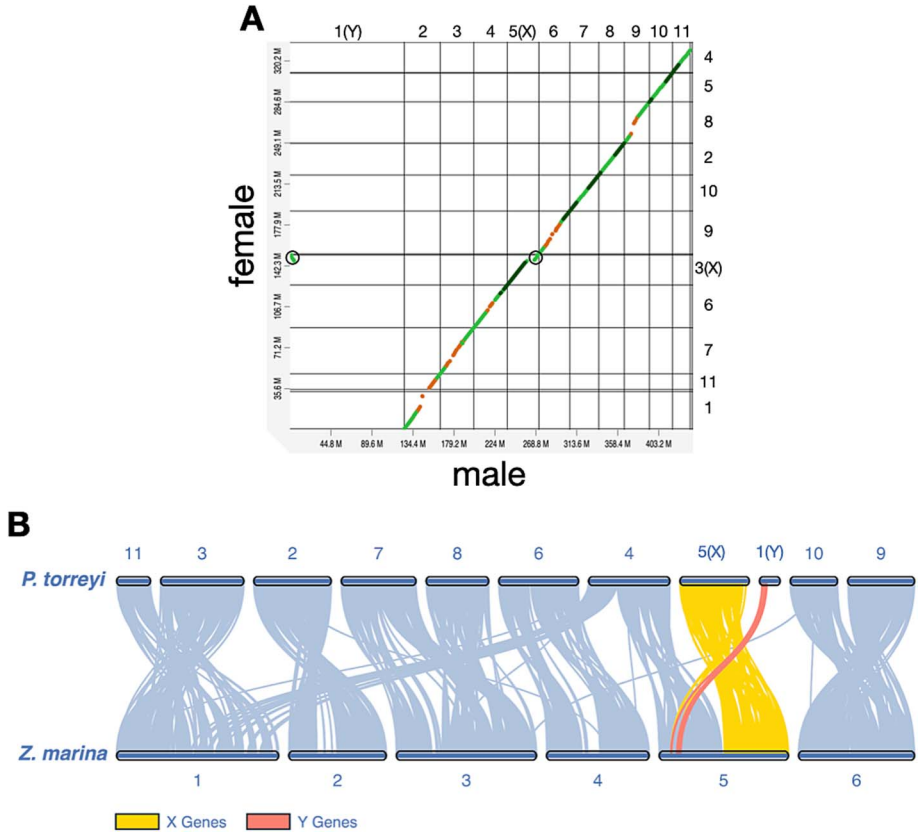

Fig. 3. Alignment of genome assemblies. A) Dot plot alignment comparing *P. Torreyi* male primary assembly and female consensus assembly. 11 chromosomes/contigs are labeled for each assembly. Chromosome 1 (Y chromosome; Pt.1) is unique to the male except for the putative PAR with the X chromosome (circled on both Pt.1 and Pt.5/Pt.3 female). B) Gene synteny blocks shared between *P. Torreyi* scaffolds and *Z. Marina* chromosomes. Yellow syntenic blocks denote genes occurring on the *P. Torreyi* X chromosome, and orange on the Y. Chromosomes (1–6 for *Z. Marina*, and 1–11 for *P. Torreyi*) scale by presence of gene coding regions and therefore do not reflect relative chromosome size.

Our analyses clarify the nature of those fusions as well as identifying large-scale rearrangements. Further, our finding that *Zostera* and *Phyllospadix* split 25 Mya is consistent with Coyer et al. (2013) who estimated the split at 23 Mya and (Silva et al. 2021), who estimated 25–45 Mya. Despite the Y chromosome of *P. torreyi* being gene-poor overall (hence why it appears so small in Fig. 3B), 139 of its 581 annotated proteins sit within syntenic blocks that are shared with *Z. marina*, underscoring substantial orthologous continuity even within sex-linked regions. The persistence of floral regulatory genes on the *P. torreyi* Y chromosomes indicates that sex linkage may have arisen through the adaptive recruitment of ancestral developmental loci, linking pre-existing meristem and organ identity pathways to the evolution of sexual dimorphism after the divergence from *Zostera*.

The near chromosome level assembly of the *P. torreyi* genome will be a powerful tool for population and landscape genomic studies across California and North America. The assembly of this genome may help reveal the genetic mechanism driving male scarcity in *P. torreyi*. Future studies should also examine the molecular dynamics of dioecy in *Phyllospadix*, including the age of origin, and whether this coincided with the split with *Zostera*, or if it happened subsequently. Further, assembling genomes for multiple *P. torreyi* individuals could help resolve whether the presence or absence of genes is fixed in the species, or if insertions/deletions occurred specifically in the individuals we sequenced.

Comparing *P. torreyi* (surfgrass) and *Z. marina* (eelgrass) offers a natural experiment in how closely related seagrasses within Zosteraceae have diverged to thrive in starkly different coastal regimes—wave-swept rocky intertidal versus sheltered soft-sediment bays. Future studies should explore the molecular mechanisms governing the adaptation to different habitats between the two lineages, and how selective pressures have shaped genome architecture, physiology, and reproductive strategy. The abundance of surfgrass, its ecological importance, and its relatively small genome size make it an efficient resource for coastal marine conservation planning and evolutionary studies.

Acknowledgments

PacBio Sequel II library prep and sequencing was carried out at the DNA Technologies and Expression Analysis Cores at the UC Davis Genome Center, supported by NIH Shared Instrumentation Grant 1S10OD010786-01. Deep sequencing of Omni-C libraries used the Novaseq S4 sequencing platforms at the Vincent J. Coates Genomics Sequencing Laboratory at UC Berkeley, supported by NIH S10 OD018174 Instrumentation Grant. We thank the staff at the UC Davis DNA Technologies and Expression Analysis Cores and the UC Santa Cruz Paleogenomics Laboratory for their diligence and dedication to generating high-quality sequence data. We particularly wish to thank Sally Holbrook, Dan Reed, Douglas Bush, and Russ Schmitt for their early inspiration and work regarding the ecological importance of

Phyllospadix and its population genetics. We thank Brian Husband for the flow cytometry analysis.

Author contributions

Jason Johns (Conceptualization, Data curation, Formal analysis, Funding acquisition, Investigation, Methodology, Project administration, Validation, Visualization, Writing—original draft, Writing—review & editing), Malia L. Moore (Conceptualization, Data curation, Formal analysis, Investigation, Methodology, Project administration, Visualization, Writing—original draft, Writing—review & editing), Todd P. Michael (Conceptualization, Funding acquisition, Investigation, Methodology, Resources, Software, Supervision, Validation, Writing—review & editing), Scott Hodges (Conceptualization, Data curation, Formal analysis, Funding acquisition, Investigation, Methodology, Project administration, Resources, Software, Supervision, Validation, Visualization, Writing—original draft, Writing—review & editing), Merly Escalona (Conceptualization, Data curation, Formal analysis, Investigation, Methodology, Software, Validation, Visualization, Writing—original draft, Writing—review & editing), Courtney Miller (Conceptualization, Data curation, Funding acquisition, Project administration, Supervision, Validation, Writing—review & editing), Noravit Chumchim (Data curation, Investigation, Methodology), Oanh Nguyen (Data curation, Investigation, Methodology), Mohan P.A. Marimuthu (Data curation, Investigation, Methodology), Colin W. Fairbairn (Data curation, Investigation, Methodology), Eric Beraut (Data curation, Investigation, Methodology), William E. Seligmann (Data curation, Investigation, Methodology), Samuel Sacco (Data curation, Formal analysis, Investigation, Methodology), Erin Toffelmier (Conceptualization, Data curation, Funding acquisition, Methodology, Project administration, Resources, Supervision), H. Bradley Shaffer (Conceptualization, Funding acquisition, Project administration, Resources, Supervision)

Supplementary material

Supplementary material is available at *Journal of Heredity* online.

Funding

This work was supported by the California Conservation Genomics Project, with funding provided to the University of California by the State of California, State Budget Act of 2019 [UC Award ID RSI-19-690224]; a National Science Foundation (NSF) graduate research fellowship [Fellow #2021321499] to M.L.M; and Tang Genomics Fund to T.P.M.

Data availability

Data generated for this study are available under NCBI BioProjects PRJNA808359 and PRJNA1237327. Raw sequencing data for sample Pt_campus_point_CCGP (NCBI BioSample SAMN41460720) are deposited in the NCBI Short Read Archive (SRA) under SRX26568932 for PacBio HiFi sequencing data, and SRR31187414, SRR31187414 for the Omni-C Illumina sequencing data; for sample Ptor311-Wns, PacBio Hifi sequencing data are deposited under SRR32736722. GenBank accessions for both primary and alternate assemblies of Pt_campus_point_CCGP are GCA_043789395.1 and GCA_043789325.1, and for genome sequences JBFLFR000000000 and JBFLFS000000000. The GenBank genome assembly for the chloroplast genome is JBFLFR010000079.1. Assembly scripts and other data for the analyses presented can be found at the following GitHub repository: www.github.com/ccgproject/ccgp_assembly

References

Abdennur N, Mirny LA. Cooler: scalable storage for hi-C data and other genomically labeled arrays. *Bioinformatics*. 2020;**36**:311–316. https://doi.org/10.1093/bioinformatics/btz540

Akagi T, Fujita N, Shirasawa K, Tanaka H, Nagaki K, Masuda K, Horiuchi A, Kuwada E, Kawai K, Kunou R, et al. Rapid and dynamic evolution of a giant Y chromosome in *Silene latifolia*. *Science*. 2025;**387**:637–643. https://doi.org/10.1126/science.adk9074

Astashyn A, Tvedte ES, Sweeney D, Sapojnikov V, Bouk N, Joukov V, Mozes E, Strope P. K, Sylla PM, Wagner L, et al. Rapid and sensitive detection of genome contamination at scale with FCS-GX. *Genome Biology*. 2024;**25**. https://doi.org/10.1186/s13059-024-03198-7

Bachtrog D. Y-chromosome evolution: emerging insights into processes of Y-chromosome degeneration. *Nat Rev Genet*. 2013;**14**:113–124. https://doi.org/10.1038/nrg3366

Bush D, Hollbrook S, Schmitt, Reed D, Hodges S. Male-specific AFLP markers reveal extreme female-biased sex-ratios in the surfgrass Phyllospadix torreyi (Zosteraceae). *Minerals Management Service, Final Study Report MMS 2006–049*. 2006;**1**:1–5

Cabanettes F, Klopp C. D-GENIES: dot plot large genomes in an interactive, efficient and simple way. *PeerJ*. 2018;**6**:e4958. https://doi.org/10.7717/peerj.4958

Camacho C, Coulouris G, Avagyan V, Ma N, Papadopoulos J, Bealer K, Madden TL. BLAST+: architecture and applications. *BMC Bioinformatics*. 2009;**10**:421. https://doi.org/10.1186/1471-2105-10-421

Cantalapiedra C, Hernández-Plaza A, Letunic I, Bork P, Huerta-Cepas J. eggNOG-mapper v2: functional annotation, orthology assignments, and domain prediction at the metagenomic scale. *Mol Bio Evol*. 2021;**38**:5825–5829. https://doi.org/10.1093/molbev/msab293

Challis R, Richards E, Rajan J, Cochrane G, Blaxter M. BlobToolKit - interactive quality assessment of genome assemblies. *G3 (Bethesda)*. 2020;**10**:1361–1374. https://doi.org/10.1534/g3.119.400908

Challis R, Kumar S, Sotero-Caio C, Brown M, Blaxter M. Genomes on a tree (GoaT): a versatile, scalable search engine for genomic and sequencing project metadata across the eukaryotic tree of life. *Wellcome Open Res*. 2023;**8**:24. https://doi.org/10.12688/wellcomeopenres.18658.1

Charlesworth B, Charlesworth D. The degeneration of Y chromosomes. *Philos Trans R Soc Lond Ser B Biol Sci*. 2000;**355**:1563–1572. https://doi.org/10.1098/rstb.2000.0717

Cheng H, Concepcion GT, Feng X, Zhang H, Li H. Haplotype-resolved de novo assembly using phased assembly graphs with hifiasm. *Nat Methods*. 2021;**18**:170–175. https://doi.org/10.1038/s41592-020-01056-5

Cox PA, Tomlinson PB, Nieznanski K. Hydrophilous pollination and reproductive morphology in the seagrassPhyllospadix scouleri (Zosteraceae). *Plant Syst Evol*. 1992;**180**:65–75. https://doi.org/10.1007/BF00940398

Coyer JA, Hoarau G, Kuo J, Tronholm A, Veldsink J, Olsen JL Phylogeny and temporal divergence of the seagrass family Zosteraceae using one nuclear and three chloroplast loci. *Systematics and Biodiversity*. 2013;**11**:271–284. https://doi.org/10.1080/14772000.2013.821187

Danecek P, Bonfield JK, Liddle J, Marshall J, Ohan V, Pollard MO, Whitwham A, Keane T, McCarthy SA, Davies RM, et al. Twelve years of SAMtools and BCFtools. *Gigascience*. 2021;**10**:1–5. https://doi.org/10.1093/gigascience/giab008

Gaut P, Morton BR, McCaig BC, Clegg MT. Substitution rate comparisons between grasses and palms: synonymous rate differences at the nuclear gene Adh parallel rate differences at the plastid gene rbcL. *Proc Natl Acad Sci USA*. 1996;**93**:10274–10279. https://doi.org/10.1073/pnas.93.19.10274

Ghurye J, Pop M, Koren S, Bickhart D, Chin CS. Scaffolding of long read assemblies using long range contact information. *BMC Genomics*. 2017;**18**:527. https://doi.org/10.1186/s12864-017-3879-z

Ghurye J, Rhie A, Walenz BP, Schmitt A, Selvaraj S, Pop M, Phillippy AM, Koren S. Integrating hi-C links with assembly graphs for chromosome-scale assembly. *PLoS Comput Biol*. 2019;**15**:e1007273. https://doi.org/10.1371/journal.pcbi.1007273

Greiner S, Lehwark P, Bock R. OrganellarGenomeDRAW (OGDRAW) version 1.3.1: expanded toolkit for the graphical visualization of

organellar genomes. *Nucleic Acids Res*. 2019;**47**:W59–W64. https://doi.org/10.1093/nar/gkz238

Gurevich A, Saveliev V, Vyahhi N, Tesler G. QUAST: quality assessment tool for genome assemblies. *Bioinformatics*. 2013;**29**:1072–1075. https://doi.org/10.1093/bioinformatics/btt086

Harada I. Sex-chromosome of Phyllospadix. *Jpn J Genet*. 1944;**20**: 127–128. https://doi.org/10.1266/jjg.20.127

Harris RS. Improved pairwise alignment of genomic DNA. 2007;1–17

Inglis PW, Pappas MCR, Resende LV, Grattapaglia D. Fast and inexpensive protocols for consistent extraction of high quality DNA and RNA from challenging plant and fungal samples for high-throughput SNP genotyping and sequencing applications. *PLoS One*. 2018;**13**:e0206085. https://doi.org/10.1371/journal.pone.0206085

Jepson eFlora. *Jepson Flora project*. 2025: https://ucjeps.berkeley.edu/eflora/.

Kerpedjiev P, Abdennur N, Lekschas F, McCallum C, Dinkla K, Strobelt H, Luber JM, Ouellette SB, Azhir A, Kumar N, et al. HiGlass: web-based visual exploration and analysis of genome interaction maps. *Genome Biol*. 2018;**19**:125. https://doi.org/10.1186/s13059-018-1486-1

Korlach J, Gedman G, Kingan SB, Chin CS, Howard JT, Audet JN, Cantin L, Jarvis ED. De novo PacBio long-read and phased avian genome assemblies correct and add to reference genes generated with intermediate and short reads. *Gigascience*. 2017;**6**:1–16. https://doi.org/10.1093/gigascience/gix085

Lee S, Bakker CR, Vitzthum C, Alver BH, Park PJ Pairs and Pairix: a file format and a tool for efficient storage and retrieval for Hi-C read pairs. *Bioinformatics*. 2022;**38**:1729–1731. https://doi.org/10.1093/bioinformatics/btab870

Li H. Aligning sequence reads, clone sequences and assembly contigs with BWA-MEM. arXiv [q-bio.GN]. 2013.

Li H. Minimap2: pairwise alignment for nucleotide sequences. *Bioinformatics*. 2018;**34**:3094–3100. https://doi.org/10.1093/bioinformatics/bty191

Li H. New strategies to improve minimap2 alignment accuracy. *Bioinformatics*. 2021;**37**:4572–4574. https://doi.org/10.1093/bioinformatics/btab705

Linnaeus C (1753) *Species plantarum, exhibentes plantas rite cognitas ad genera relatas cum differentiis specificis, nominibus trivialibus, synonymis selectis, locis natalibus, secundum systema sexuale digestas*. Salvius, Stockholm, https://doi.org/10.5962/bhl.title.669

Manni M, Berkeley MR, Seppey M, Simão FA, Zdobnov EM BUSCO update: novel and streamlined workflows along with broader and deeper phylogenetic coverage for scoring of eukaryotic, prokaryotic, and viral genomes. 2021a;**38**:4647–4654.

Manni M, Berkeley MR, Seppey M, Zdobnov EM. BUSCO: assessing genomic data quality and beyond. *Curr Protoc*. 2021b;**1**:e323. https://doi.org/10.1002/cpz1.323

Ma X, Olsen JL, Reusch TBH, Procaccini G, Kudrna D, Williams M, Grimwood J, Rajasekar S, Jenkins J, Schmutz J, et al. Improved chromosome-level genome assembly and annotation of the seagrass, Zostera marina (eelgrass). *F1000Res*. 2021;**10**:289. https://doi.org/10.12688/f1000research.38156.1

McMillan C, Phillips RC, Phillips RC. Morphological variation and isozymes of north American Phyllospadix (Potamogetonaceae). *Can J Bot*. 1981;**59**:1494–1500. https://doi.org/10.1139/b81-203

Moraga C, Branco C, Rougemont Q, Jedlička P, Mendoza-Galindo E, Veltsos P, Hanique M, Rodríguez de la Vega RC, Tannier E, Liu X, et al. The Silene latifolia genome and its giant Y chromosome. *Science*. 2025;**387**:630–636. https://doi.org/10.1126/science.adj7430

Mtwana Nordlund L, Koch EW, Barbier EB, Creed JC. Seagrass ecosystem services and their variability across genera and geographical regions. *PLoS One*. 2016;**11**:e0163091. https://doi.org/10.1371/journal.pone.0163091

Olsen JL, Rouzé P, Verhelst B, Lin Y-C, Bayer T, Collen J, Dattolo E, De Paoli E, Dittami S, Maumus F, et al. The genome of the seagrass Zostera marina reveals angiosperm adaptation to the sea. *Nature*. 2016;**530**:331–335. https://doi.org/10.1038/nature16548

Open2C, Abdennur N, Fudenberg G, Flyamer IM, Galitsyna AA, Goloborodko A, Imakaev M, Venev SV. Pairtools: from sequencing data to chromosome contacts. *PLoS Comput Biol*. 2024;**20**:e1012164

Phillips RC. Ecological notes on Phyllospadix (potamogetonaceae) in the Northeast Pacific. *Aquat Bot*. 1979;**6**:159–170. https://doi.org/10.1016/0304-3770(79)90059-7

Pockrandt C, Alzamel M, Iliopoulos CS, Reinert K. GenMap: ultra-fast computation of genome mappability. *Bioinformatics*. 2020;**36**: 3687–3692. https://doi.org/10.1093/bioinformatics/btaa222

Poplin R, Chang PC, Alexander D, Schwartz S, Colthurst T, Ku A, Newburger D, Dijamco J, Nguyen N, Afshar PT, et al. A universal SNP and small-indel variant caller using deep neural networks. *Nat Biotechnol*. 2018;**36**:983–987. https://doi.org/10.1038/nbt.4235

Quinlan AR, Hall IM. BEDTools: a flexible suite of utilities for comparing genomic features. *Bioinformatics*. 2010;**26**:841–842. https://doi.org/10.1093/bioinformatics/btq033

Ramírez F, Bhardwaj V, Arrigoni L, Lam KC, Grüning BA, Villaveces J, Habermann B, Akhtar A, Manke T. High-resolution TADs reveal DNA sequences underlying genome organization in flies. *Nat Commun*. 2018;**9**:189. https://doi.org/10.1038/s41467-017-02525-w

Ranallo-Benavidez TR, Jaron KS, Schatz MC. GenomeScope 2.0 and Smudgeplot for reference-free profiling of polyploid genomes. *Nat Commun*. 2020;**11**:1432. https://doi.org/10.1038/s41467-020-14998-3

Rhie A, McCarthy SA, Fedrigo O, Damas J, Formenti G, Koren S, Uliano-Silva M, Chow W, Fungtammasan A, Kim J, et al. Towards complete and error-free genome assemblies of all vertebrate species. *Nature*. 2021;**592**:737–746. https://doi.org/10.1038/s41586-021-03451-0

Rhie A, Walenz BP, Koren S, Phillippy AM. Merqury: reference-free quality, completeness, and phasing assessment for genome assemblies. *Genome Biol*. 2020;**21**:245. https://doi.org/10.1186/s13059-020-02134-9

Sabara A, Kron P, Husband B. Cytochroms coexistence leads to triploid hybrid production in a diploid-tetrapoloid contact zone of Chamerion angustifolium (Onagraceae). *Am J Bot*. 2013;**100**(5):962–970. https://doi.org/10.3732/ajb.1200583

Sacchi B, Humphries Z, Kružlicová J, Bodláková M, Pyne C, Choudhury BI, Gong Y, Bačovský V, Hobza R, Barrett S. C. H, et al. Phased Assembly of Neo-Sex Chromosomes Reveals Extensive Y Degeneration and Rapid Genome Evolution in Rumex hastatulus. *Molecular Biology and Evolution*. 2024;**41**. https://doi.org/10.1093/molbev/msae074

Sato S, Nakamura Y, Kaneko T, Asamizu E, Tabata S. Complete structure of the chloroplast genome of Arabidopsis thaliana. *DNA Res*. 1999;**6**:283–290. https://doi.org/10.1093/dnares/6.5.283

Shaffer HB, Toffelmier E, Corbett-Detig RB, Escalona M, Erickson B, Fiedler P, Gold M, Harrigan RJ, Hodges S, Luckau TK, et al. Landscape genomics to enable conservation actions: the California conservation genomics project. *J Hered*. 2022;**113**:577–588. https://doi.org/10.1093/jhered/esac020

She H, Liu Z, Xu Z, Zhang H, Wu J, Wang X, Cheng F, Charlesworth D, Qian W. Genome sequence of the wild species, Spinacia tetrandra, including a phased sequence of the extensive sex-linked region, revealing partial degeneration in evolutionary strata with unusual properties. *New Phytol*. 2025;**246**(6):2765–2781. https://doi.org/10.1111/nph.70165

Shelton AO. Temperature and community consequences of the loss of foundation species: Surfgrass (Phyllospadix spp., hooker) in tidepools. *J Exp Mar Bio Ecol*. 2010a;**391**:35–42. https://doi.org/10.1016/j.jembe.2010.06.003

Shelton AO. Skewed sex ratios, pollen limitation, and reproductive failure in the dioecious seagrass phyllospadix. *Ecology*. 2008;**89**: 3020–3029. https://doi.org/10.1890/07-1835.1

Shelton AO. The origin of female-biased sex ratios in intertidal seagrasses (Phyllospadix spp.). *Ecology*. 2010b;**91**:1380–1390. https://doi.org/10.1890/09-0685.1

Silva, S. L. da, Carvalho, Rde, & Magalhães KM Chromosomal evolution in seagrasses: Is the chromosome number decreasing? *Aquatic Botany*. 2021;**173**:103410. https://doi.org/10.1016/j.aquabot.2021.103410

Sim SB, Corpuz RL, Simmonds TJ, Geib SM HiFiAdapterFilt, a memory efficient read processing pipeline, prevents occurrence of adapter sequence in PacBio HiFi reads and their negative impacts on genome assembly. *BMC Genomics*. 2022;**23**. https://doi.org/10.1186/s12864-022-08375-1

Stiehler F, Steinborn M, Scholz S, Dey D, Weber APM, Denton AK Helixer: cross-species gene annotation of large eukaryotic genomes using deep learning. *Bioinformatics*. 2020;**36**:5291–5298. https://doi.org/10.1093/bioinformatics/btaa1044

Stewart JG, Rüdenberg, L. MICROSPOROCYTE GROWTH AND MEIOSIS IN PHYLLOSPADIX TORREYI, A MARINE MONOCOTYLEDON. *American Journal of Botany*. 1980;**67**:949–954. Portico. https://doi.org/10.1002/j.1537-2197.1980.tb07725.x

Tillich M, Lehwark P, Pellizzer T, Ulbricht-Jones ES, Fischer A, Bock R, Greiner S. GeSeq - versatile and accurate annotation of organelle genomes. *Nucleic Acids Res*. 2017;**45**:W6–W11. https://doi.org/10.1093/nar/gkx391

Wang Y, Tang H, Wang X, Sun Y, Joseph PV, Paterson AH Detection of colinear blocks and synteny and evolutionary analyses based on utilization of MCScanX. *Nature Protocols*. 2024;**19**:2206–2229. https://doi.org/10.1038/s41596-024-00968-2

Watson S. Phyllospadix torreyi. *Proc Am Acad Arts Sci xiv*. 1879;**303**:200–203.

Williams SL. Surfgrass (Phyllospadix Torreyi) reproduction: reproductive phenology, resource allocation, and male rarity. *Ecology*. 1995;**76**:1953–1970. https://doi.org/10.2307/1940726

Wilson MD, Riemer C, Martindale DW, Schnupf P, Boright AP, Cheung TL, Hardy DM, Schwartz S, Scherer SW, Tsui LC, et al. Comparative analysis of the gene-dense ACHE/TFR2 region on human chromosome 7q22 with the orthologous region on mouse chromosome 5. *Nucleic Acids Res*. 2001;**29**:1352–1365. https://doi.org/10.1093/nar/29.6.1352

Workman R, W Timp, R Fedak, D Kilburn, S Hao, K Liu High molecular weight DNA extraction from recalcitrant plant species for third generation sequencing. 2018.

Zhang C, Wang J, Long M, Fan C gKaKs: the pipeline for genome-level Ka/Ks calculation. *Bioinformatics*. 2013;**29**:645–646. https://doi.org/10.1093/bioinformatics/btt009

Zhou C, Brown M, Blaxter M, Darwin Tree of Life Project Consortium, McCarthy SA, Durbin R. Oatk: a de novo assembly tool for complex plant organelle genomes. 2024. https://doi.org/10.1101/2024.10.23.619857

Journal of Heredity, 2026, 117, 566–576
https://doi.org/10.1093/jhered/esaf097
Genome Resources